



HAL
open science

Stability of a class of delayed port-Hamiltonian systems with application to microgrids with distributed rotational and electronic generation

Johannes Schiffer, Emilia Fridman, Roméo Ortega, Jörg Raisch

► To cite this version:

Johannes Schiffer, Emilia Fridman, Roméo Ortega, Jörg Raisch. Stability of a class of delayed port-Hamiltonian systems with application to microgrids with distributed rotational and electronic generation. *Automatica*, 2016, 74, pp.71-79. 10.1016/j.automatica.2016.07.022 . hal-01633779

HAL Id: hal-01633779

<https://centralesupelec.hal.science/hal-01633779>

Submitted on 23 Jun 2020

HAL is a multi-disciplinary open access archive for the deposit and dissemination of scientific research documents, whether they are published or not. The documents may come from teaching and research institutions in France or abroad, or from public or private research centers.

L'archive ouverte pluridisciplinaire **HAL**, est destinée au dépôt et à la diffusion de documents scientifiques de niveau recherche, publiés ou non, émanant des établissements d'enseignement et de recherche français ou étrangers, des laboratoires publics ou privés.

Stability of a class of delayed port-Hamiltonian systems with application to microgrids with distributed rotational and electronic generation

Johannes Schiffer^{a,*}, Emilia Fridman^b, Romeo Ortega^c, Jörg Raisch^d

^a*School of Electronic and Electrical Engineering, University of Leeds, Leeds LS2 9JT, UK*

^b*Tel Aviv University, Tel Aviv 69978, Israel*

^c*Laboratoire des Signaux et Systèmes, École Supérieure d'Electricité (SUPELEC), Gif-sur-Yvette 91192, France*

^d*Technische Universität Berlin, Einsteinufer 11, 10587 Berlin, Germany and Max-Planck-Institut für Dynamik komplexer technischer Systeme, Sandtorstr. 1, 39106 Magdeburg, Germany*

Abstract

Motivated by the problem of stability in droop-controlled microgrids with delays, we consider a class of port-Hamiltonian systems with delayed interconnection matrices. For this class of systems, delay-dependent stability conditions are derived via the Lyapunov-Krasovskii method. The theoretical results are applied to an exemplary microgrid with distributed rotational and electronic generation and illustrated via a simulation example. The stability analysis is complemented by providing an estimate of the region of attraction of a microgrid with delays.

Keywords: microgrid control, microgrid stability, smart grid applications, droop control, port-Hamiltonian systems, time delay systems, Lyapunov-Krasovskii functionals

1. Introduction

1.1. Motivation

Time delays are a highly relevant phenomenon in many engineering applications. They appear, e.g., in networked control, sampled-data and biological systems [6]. In particular, time delays may substantially deteriorate the performance of a system, e.g., with regards to stability properties of its equilibria. Therefore, it is of paramount importance in a large variety of applications to explicitly consider time delays in the system design and analysis process.

In this paper, we derive conditions for stability of a class of port-Hamiltonian (pH) systems with delays. pH systems theory provides a systematic framework for modeling and analysis of network models of a large range of physical systems and processes [30, 31]. In particular, the geometric structure of a pH model underscores the importance of the energy function, the interconnection pattern and the dissipation of a system. With regards to stability analysis, the main advantage of a pH representation is that the Hamiltonian usually is a natural candidate Lyapunov function [30]. Unfortunately, in the presence of delays this

does not apply in general. Yet, it seems natural to seek to construct alternative Lyapunov function candidates by using the Hamiltonian as a point of departure aiming to exploit the structural properties of pH systems.

The present work is further motivated by the problem of the effect of time delays on microgrid (μG) operation. The μG is an emerging concept for an efficient integration of renewable distributed generation (DG) units [11, 13]. A μG is a locally controllable subset of a larger electrical network and is composed of several DG units, storage devices and loads [11]. A particular characteristic of a μG is that it can be operated either in grid-connected or in islanded mode, i.e., disconnected from a larger power system.

Typically, a large share of the power units in a μG are renewable and storage units connected to the network via DC/AC inverters. On the contrary, most conventional generation units are interfaced to the grid via synchronous generators (SGs). As inverters possess significantly different physical properties from SGs, many challenging problems arise in future power grids [13, 11]. Amongst these, system stability is one of the most relevant and critical [11].

So far, most stability analysis of μG s has focussed on purely inverter-based μG s [37, 34, 24]. Yet, from a practical point of view, most present and near-future applications concern μG s with a mixed generation pool consisting of SG- and inverter-interfaced units. Following [33], we refer to such a system as a μG with distributed rotational and electronic generation (MDREG). The predominant type of conventional units in MDREGs are diesel gensets [16] and,

*Corresponding author J. Schiffer. Tel. +44-113-3439719. Fax +44-113-3432032.

**This work was partially supported by Israel Science Foundation (Grant No. 1128/14)

Email addresses: j.schiffer@leeds.ac.uk (Johannes Schiffer), emilia@eng.tau.ac.il (Emilia Fridman), ortega@lss.supelec.fr (Romeo Ortega), raisch@control.tu-berlin.de (Jörg Raisch)

hence, we focus on these in the present work.

The most commonly employed control scheme to operate MDREGs is droop control. This is a decentralized proportional control scheme, the main objectives of which are stability and power sharing. Droop control is the standard basic control scheme for SG-based networks [19] and has also been adapted to inverter-interfaced units [11]. As shown, e.g., in [33], droop control ensures a compatible joint operation of SG- and inverter-interfaced DG units.

In MDREGs, time delays appear due to several reasons and also in several network components. First, the power-stroke and ignition delay of a diesel engine is represented by a time delay in standard models [28, 12, 17]. Second, in a practical setup, the droop control scheme is applied to an inverter, respectively an SG, via digital control. Digital control usually introduces additional effects such as clock drifts [35] and time delays [18, 23, 25], which may have a deteriorating impact on the system performance. According to [25], the main reasons for the appearance of time delays are sampling of control variables and calculation time of the digital controller. In the case of inverters, the generation of the pulse-width-modulation (PWM) to determine the switching signals for the inverter induces an additional delay. We refer the reader to, e.g., [25] for further details. Hence, time delays are a relevant phenomenon in MDREGs, which makes it important to investigate their influence on stability. This motivates the analysis below.

1.2. About the paper

The present paper focusses on the impact of time delays on stability of MDREGs. To that end, and following [34, 32], we represent the MDREG as a pH system with delays. Motivated by this, we derive delay-dependent conditions for stability for a class of pH systems with delays, containing the MDREG model as a special case. The stability conditions are established by following [8, 7, 15] and constructing a *nonlinear and non-quadratic* Lyapunov-Krasovskii functional (LKF) from the Hamiltonian and its gradient. That the LKF can be nonlinear and non-quadratic follows from the fact that both the Hamiltonian and its gradient are, in general, nonlinear functions of the system states. Compared to that, standard LMI-based approaches [7, 6] rely on LKFs, which are quadratic in the state variables. The latter is, in general, very restrictive.

The main contributions of the present paper are (i) to introduce a model of a droop-controlled MDREG which explicitly considers delays of the DG unit dynamics, (ii) to represent this MDREG model as a pH system with fast- and slowly-varying delays, (iii) to provide stability conditions for a class of pH systems with fast- and slowly-varying delays via the LK method, (iv) to provide an estimate of the region of attraction of an MDREG with delays and (v) to illustrate the usefulness of our conditions on an exemplary μ G. Hence, the present paper extends our previous work [32] in several regards: we take diesel engines into account, provide stability conditions for slowly- and

fast-varying delays and derive an estimate of the region of attraction of an MDREG with delays.

1.3. Existing literature

Stability analysis of pH systems with delays has been the subject of previous research [27, 38, 15, 2, 1]. The main motivation of that work is a scenario in which several pH systems are interconnected via feedback paths which exhibit a delay. This setup yields a closed-loop system with skew-symmetric interconnections, which can be split into non-delayed skew-symmetric and delayed skew-symmetric parts. However, the model of an MDREG with delays derived in this work is not comprised in the class of pH systems studied in [27, 38, 15, 2], since the delays do not appear skew-symmetrically. In that regard, the class of systems considered in the present work generalizes the class studied in [27, 38, 15, 2], see Section 3. Unlike [27, 15, 2], we also provide conditions for stability in the presence of fast-varying delays, which typically arise in the context of digital control [20, 7]. In addition, we apply the derived approach to a practically relevant application, namely an MDREG. Compared to this, in [27, 38, 15, 2] only academic examples were considered. The effect of time delays on μ G stability has only been investigated in [4, 5] for a two-inverter-scenario. In particular, none of the aforementioned analyses on μ G stability [37, 34, 24, 33] take the effect of time delays into account.

The remainder of the paper is structured as follows. A model of an MDREG with delays is derived in Section 2. In Section 3, the considered class of pH systems with delays is introduced, for which delay-dependent conditions for stability are provided in Section 4. In Section 5, the results are applied to an exemplary MDREG for which we also provide an estimate of the region of attraction. Conclusions and topics of future work are given in Section 6.

Notation. We define the sets $\bar{n} = \{1, 2, \dots, n\}$, $\mathbb{R}_{\geq 0} = \{x \in \mathbb{R} | x \geq 0\}$, $\mathbb{R}_{> 0} = \{x \in \mathbb{R} | x > 0\}$, $\mathbb{R}_{< 0} = \{x \in \mathbb{R} | x < 0\}$, $\mathbb{Z}_{\geq 0} = \{0, 1, 2, \dots\}$. For a set \mathcal{V} , let $|\mathcal{V}|$ denote its cardinality. For a set of, possibly unordered, positive natural numbers $\mathcal{V} = \{l, k, \dots, n\}$, the short-hand $i \sim \mathcal{V}$ denotes $i = l, k, \dots, n$. Let $x = \text{col}(x_i) \in \mathbb{R}^n$ denote a vector with entries x_i for $i \sim \bar{n}$, $\mathbf{0}_n$ the zero vector, $\mathbf{1}_n$ the vector with all entries equal to one, I_n the $n \times n$ identity matrix, $\mathbf{0}_{n \times n}$ the $n \times n$ matrix with all entries equal to zero and $\text{diag}(a_i), i \sim \bar{n}$, an $n \times n$ diagonal matrix with diagonal entries $a_i \in \mathbb{R}$. Likewise, $A = \text{blkdiag}(A_i)$ denotes a block-diagonal matrix with matrix entries A_i . We employ the notation $\mathcal{I}_{n \times mn} = [I_n, \dots, I_n] \in \mathbb{R}^{n \times mn}$. For $A \in \mathbb{R}^{n \times n}$, $A > 0$ means that A is symmetric positive definite. The elements below the diagonal of a symmetric matrix are denoted by $*$. We denote by $W[-h, 0]^n$, $h \in \mathbb{R}_{> 0}$, the Banach space of absolutely continuous functions $\phi : [-h, 0] \rightarrow \mathbb{R}^n$, $h \in \mathbb{R}_{> 0}$, with $\dot{\phi} \in L_2(-h, 0)^n$ and with the norm $\|\phi\|_W = \max_{\theta \in [a, b]} |\phi(\theta)| + \left(\int_{-h}^0 \dot{\phi}^2 d\theta \right)^{0.5}$. For $x : \mathbb{R}_{\geq 0} \rightarrow \mathbb{R}^n$, we denote $x_t(\sigma) = x(t + \sigma)$, $\sigma \in [-h, 0]$. Also, ∇f denotes the transpose of the gradient of a function $f : \mathbb{R}^n \rightarrow \mathbb{R}$,

$\nabla^2 H$ its Hessian matrix and we employ the notation $\nabla \dot{f} = d(\nabla f)/dt$. If f takes the form $f = f(x(t-h))$, $x \in \mathbb{R}^n$, we use the short-hand $\nabla f_h = \nabla f(x(t-h))$.

2. Motivating application: microgrids with distributed rotational and electronic generation

2.1. Network model

We consider a Kron-reduced [19] generic MDREG in which DG units are interfaced to the network either via SGs or inverters and loads are modeled by constant impedances. The network is composed of $n_1 \geq 1$ inverters and $n_2 \geq 1$ SGs and the set of network nodes is denoted by $\bar{n} = \bar{n}_1 \cup \bar{n}_2$ with $\bar{n}_1 = \{1, \dots, n_1\}$, $\bar{n}_2 = \{n_1 + 1, \dots, n\}$ and $n = n_1 + n_2$. Following [37, 34], we assume that the line admittances are purely inductive. Then, two nodes i and k in the network are connected by a nonzero susceptance $B_{ik} \in \mathbb{R}_{<0}$. We denote the set of neighbors of the i -th node by $\hat{n}_i = \{k \in \bar{n} \mid B_{ik} \neq 0\}$, associate a time-dependent phase angle $\delta_i : \mathbb{R}_{\geq 0} \rightarrow \mathbb{R}$ to each node $i \in \bar{n}$ and use the short-hand $\delta_{ik}(t) = \delta_i(t) - \delta_k(t)$, $i \in \bar{n}$, $k \in \bar{n}$.

In addition, we conduct our analysis under the frequent assumption of constant voltage amplitudes $V_i \in \mathbb{R}_{>0}$ at all nodes $i \in \bar{n}$, see, e.g., [37]. The active power injection $P_i : \mathbb{R}^n \rightarrow \mathbb{R}$ of the i -th inverter is then given by [19]¹

$$P_i(\delta_1, \dots, \delta_n) = G_{ii}V_i^2 + \sum_{i \sim \bar{n}_i} a_{ik} \sin(\delta_{ik}), \quad (2.1)$$

where $a_{ik} = |B_{ik}|V_iV_k > 0$ and $G_{ii} \in \mathbb{R}_{\geq 0}$ denotes the shunt conductance (representing the load) at the i -th node².

Finally, we assume that the μ G is connected, i.e., for all pairs $(i, k) \in \bar{n} \times \bar{n}$, $i \neq k$, there exists an ordered sequence of nodes from i to k such that any pair of consecutive nodes in the sequence is connected by a power line.

2.2. Inverter model with input delay

Usually, inverter-based DG units are controlled via digital control [25]. As discussed in Section 1, this leads to an input delay. In MDREGs, these delays are heterogeneous, as not all inverters are identical with respect to their hardware and the implementation of the digital controls.

Typically, the delay induced by digital control is composed of two main parts: a constant delay $\eta \in \mathbb{R}_{>0}$ originating from the calculation time of the control signal³ and the PWM and an additional delay caused by the sample-and-hold function of control variables [25]. Following [20,

6], we assume that the sampling intervals are bounded, i.e., $t_{\kappa+1} - t_\kappa \leq h_s$, $\kappa \in \mathbb{Z}_{\geq 0}$. Then,

$$t_{\kappa+1} - t_\kappa + \eta \leq h_s + \eta = \bar{h}, \quad (2.2)$$

where \bar{h} denotes the maximum time interval between the time $t_\kappa - \eta$, where the measurement is sampled and the time $t_{\kappa+1}$, where the next control input update arrives.

By following [20, 6] and [35], the inverter at the i -th node, $i \in \bar{n}_1$, with input delay and zero-order-hold update characteristic with sampling instants $t_{i,\kappa}$, $\kappa \in \mathbb{Z}_{\geq 0}$ can be represented for $t_{i,\kappa} \leq t < t_{i,\kappa+1}$, $\kappa \in \mathbb{Z}_{\geq 0}$ by⁴

$$\begin{aligned} \dot{\delta}_i(t) &= u_i^\delta(t_{i,\kappa} - \eta_i), \\ \tau_{P_i} \dot{P}_i^m(t) &= -P_i^m(t) + P_i(t), \end{aligned} \quad (2.3)$$

where $u_i^\delta : \mathbb{R}_{\geq 0} \rightarrow \mathbb{R}$ is the control input, $\eta_i \in \mathbb{R}_{>0}$ is a constant delay, P_i is given by (2.1), $P_i^m : \mathbb{R}_{\geq 0} \rightarrow \mathbb{R}$ is the measured active power and $\tau_{P_i} \in \mathbb{R}_{>0}$ is the time constant of the measurement filter. We assume that the inverters are controlled via the usual frequency droop control [11]

$$u_i^\delta(t) = \omega^d - k_{P_i}(P_i^m(t) - P_i^d), \quad (2.4)$$

where $\omega^d \in \mathbb{R}_{>0}$ is the desired (nominal) network frequency, $k_{P_i} \in \mathbb{R}_{>0}$ is the feedback (or droop) gain and $P_i^d \in \mathbb{R}_{>0}$ is the desired active power setpoint.

2.3. Diesel genset with fuel actuator and engine delay

The most common type of SG-interfaced DG units in μ Gs are diesel gensets [16]. A typical diesel genset consists of a diesel engine with fuel actuator, an SG, as well as speed and excitation controls. Based on [28, 12, 17], the dynamics of the SG with fuel actuator at the i -th node, $i \in \bar{n}_2$, are given for $t_{i,\kappa} \leq t < t_{i,\kappa+1}$, $\kappa \in \mathbb{Z}_{\geq 0}$ by

$$\begin{aligned} \dot{\delta}_i(t) &= \omega_i(t), \\ M_i \dot{\omega}_i(t) &= -D_i \omega_i(t) - P_i(t) + P_{M_i}(t), \\ \tau_{M_i} \dot{\Phi}_i(t) &= -\Phi_i(t) + k_{M_i} u_i^M(t_{i,\kappa} - \eta_i), \\ P_{M_i}(t) &= k_{c_i} \Phi_i(t - g_i(t)), \end{aligned} \quad (2.5)$$

where $\omega_i : \mathbb{R}_{\geq 0} \rightarrow \mathbb{R}$ is the frequency of the SG, $M_i \in \mathbb{R}_{>0}$ its inertia constant, $D_i \in \mathbb{R}_{>0}$ its damping coefficient, P_i the active power given by (2.1) and $P_{M_i} : \mathbb{R}_{\geq 0} \rightarrow \mathbb{R}$ the mechanical power input. The fuel actuator is represented by a first-order filter with input $u_i^M : \mathbb{R}_{\geq 0} \rightarrow \mathbb{R}$, output $\Phi_i : \mathbb{R}_{\geq 0} \rightarrow \mathbb{R}$ (the fuel flow), gain $k_{M_i} \in \mathbb{R}_{>0}$ and time constant $\tau_{M_i} \in \mathbb{R}_{>0}$. As in (2.3), we assume that the implementation of the digital control leads to an input delay and zero-order-hold update characteristic with sampling instants $t_{i,\kappa}$, $\kappa \in \mathbb{Z}_{\geq 0}$ and constant delay $\eta_i \in \mathbb{R}_{>0}$, see [12]. The fuel conversion gain is denoted by

¹To simplify notation the time argument of all signals is omitted, whenever clear from the context.

²For constant voltage amplitudes, any constant power load can equivalently be represented by a constant impedance load.

³The delay η may also represent the dynamics of the internal control system of the inverter, which is not considered explicitly in the model (2.7). See [36] for a detailed model derivation of the non-delayed version of (2.7).

⁴An underlying assumption to this model is that whenever the inverter connects a fluctuating renewable generation source to the grid, it is equipped with some sort of storage, see [36].

$k_{c_i} \in \mathbb{R}_{>0}$. The conversion process is additionally affected by the power-stroke and ignition delay, caused by the discrete firing of the cylinders, as well as the period of time between the start of injection and the start of combustion [28, 17]. This delay is, in general, considered as an uncertain constant [12] or time-varying bounded parameter [28, 17]. Hence, for the sake of generality, it is represented by a slowly-varying bounded time delay $g_i : \mathbb{R}_{\geq 0} \rightarrow [0, \bar{g}_i]$, $\bar{g}_i \in \mathbb{R}_{>0}$, $\dot{g}_i \leq d_i < 1$, $d_i \in \mathbb{R}_{>0}$ in the present paper.

As usual, we assume that the engine speed is controlled via the well-known droop control for SGs given by [33]

$$u_i^M(t) = P_i^d - R_i^{-1}(\omega_i(t) - \omega^d), \quad (2.6)$$

where $P_i^d \in \mathbb{R}_{>0}$ is the nominal power setpoint, $R_i \in \mathbb{R}_{>0}$ the droop gain and, as in (2.4), $\omega^d \in \mathbb{R}_{>0}$ the reference frequency. Since we assume constant voltage amplitudes, the excitation control is neglected in the model.

2.4. Closed-loop MDREG model

It has been shown in [20, 6] that the type of delay appearing in the open-loop systems (2.3) and (2.5) results in a fast-varying delay, once the loop is closed. Following [20, 6], we define $h_i(t) = t - t_{i,\kappa} + \eta_i$, $t_{i,\kappa} \leq t < t_{i,\kappa+1}$. Combining (2.3) with (2.4), yields the closed-loop system

$$\begin{aligned} \dot{\delta}_i(t) &= \omega^d - k_{P_i}(P_i^m(t - h_i(t)) - P_i^d), \\ \tau_{P_i} \dot{P}_i^m(t) &= -P_i^m(t) + P_i(t). \end{aligned} \quad (2.7)$$

Note that (2.2) implies that $\eta_i \leq h_i(t) \leq t_{i,\kappa+1} - t_{i,\kappa} + \eta_i \leq \bar{h}_i$ and $\dot{h}_i(t) = 1$. As standard in sampled-data networked control systems [9, 7], the delay h_i is piecewise-continuous. Via the affine state transformation (see [33, 34])

$$\begin{bmatrix} \delta_i \\ \omega_i \end{bmatrix} = \begin{bmatrix} 1 & 0 \\ 0 & -k_{P_i} \end{bmatrix} \begin{bmatrix} \delta_i \\ P_i^m \end{bmatrix} + \begin{bmatrix} 0 & 0 \\ 0 & 1 \end{bmatrix} \begin{bmatrix} 0 \\ \omega^d + k_{P_i} P_i^d \end{bmatrix},$$

we write the system (2.7), (2.4) as

$$\begin{aligned} \dot{\delta}_i(t) &= \omega_i(t - h_i(t)), \\ \tau_{P_i} \dot{\omega}_i(t) &= -\omega_i(t) + \omega^d - k_{P_i}(P_i(t) - P_i^d). \end{aligned} \quad (2.8)$$

By combining (2.5) and (2.6), the closed-loop system of the diesel genset with fast-varying delay h_i and slowly-varying delay g_i at the i -th node, $i \in \bar{n}_2$, is given by

$$\begin{aligned} \dot{\delta}_i(t) &= \omega_i(t), \\ M_i \dot{\omega}_i(t) &= -D_i \omega_i(t) - P_i(t) + k_{c_i} \Phi_i(t - g_i(t)), \\ \tau_{M_i} \dot{\Phi}_i(t) &= -\Phi_i(t) + k_{M_i}(P_i^d - R_i^{-1}(\omega_i(t - h_i(t)) - \omega^d)), \end{aligned} \quad (2.9)$$

with $\eta_i \leq h_i(t) \leq t_{i,\kappa+1} - t_{i,\kappa} + \eta_i \leq \bar{h}_i$ and $\dot{h}_i(t) = 1$.

2.5. Synchronized motion and error states

It is convenient to introduce the notion of a desired synchronized motion.

Definition 2.1. A solution $\text{col}(\delta^s, \omega^s \mathbb{1}_n, \Phi^s) \in \mathbb{R}^{(2n+n_2)}$ of the system (2.1), (2.8), (2.9), $i \sim \bar{n}$, is a desired synchronized motion if ω^s and Φ^s are constant and $\delta^s \in \Theta$, where

$$\Theta = \left\{ \delta(t) \in \mathbb{R}^n \mid |\delta_{ik}| < \frac{\pi}{2}, i \sim \bar{n}, k \sim \hat{n}_i \right\},$$

such that $\delta_{ik}^s = \delta_i^s - \delta_k^s$ are constant, $i \sim \bar{n}$, $k \sim \hat{n}_i$, $\forall t \geq 0$.

Remark 2.2. It can be shown that the system (2.1), (2.8), (2.9) possesses at most one synchronized motion (modulo a uniform shift in δ^s), see [3, Corollary 1].

For our subsequent analysis, we make the following natural power-balance feasibility assumption, see also [34].

Assumption 2.3. The system (2.1), (2.8), (2.9), $i \sim \bar{n}$, possesses a desired synchronized motion.

We denote the vector of phase angles by $\delta = \text{col}(\delta_i) \in \mathbb{R}^n$, the vector of frequencies $\omega_i = \dot{\delta}_i$ by $\omega = \text{col}(\omega_i) \in \mathbb{R}^n$ and the vector of fuel flows by $\Phi \in \mathbb{R}^{n_2}$. Note that the power flows (2.1) only depend upon angle differences. Hence, under Assumption 2.3, we introduce the error states

$$\begin{aligned} \tilde{\omega}(t) &= \omega(t) - \omega^s \mathbb{1}_n \in \mathbb{R}^n, \quad \tilde{\Phi}(t) = \Phi(t) - \Phi^s \in \mathbb{R}^{n_2}, \\ \theta(t) &= \mathcal{C}(\delta(0) - \delta^s(0) + \int_0^t \tilde{\omega}(\tau) d\tau) \in \mathbb{R}^{(n-1)}, \\ \mathcal{C} &= [I_{(n-1)} \quad -\mathbb{1}_{(n-1)}] \in \mathbb{R}^{(n-1) \times n}, \end{aligned}$$

where we have expressed all angles relative to an arbitrary reference node, here node n . For ease of notation, we define the constant $\theta_n = 0$, which is not part of θ . In the reduced coordinates, the power flows (2.1) between nodes are given by

$$P_i(\delta(\theta)) = \sum_{k \sim \hat{n}_i} a_{ik} \sin(\theta_{ik} + \delta_{ik}^s). \quad (2.10)$$

Furthermore, by introducing $\tau_{P_k} = M_k D_k^{-1}$, $k_{P_k} = D_k^{-1}$, $c_l = \omega^d - \omega^s + k_{P_l}(P_l^d - G_{ll} V_l^2)$, $c_k = -\omega^s - k_{P_k} G_{kk} V_k^2 + k_{c_k} k_{P_k} \Phi_k^s$, $c = \text{col}(c_i) \in \mathbb{R}^n$ with $i \sim \bar{n}$, $l \sim \bar{n}_1$, $k \sim \bar{n}_2$, as well as the matrices

$$\begin{aligned} K_P &= \text{diag}(k_{P_i}) \in \mathbb{R}^{n \times n}, \quad T_P = \text{diag}(\tau_{P_i}) \in \mathbb{R}^{n \times n}, \\ E &= \begin{bmatrix} 0_{n_1 \times n_2} \\ I_{n_2} \end{bmatrix} \in \mathbb{R}^{n \times n_2}, \quad K_C = \text{diag}(k_{c_k}) \in \mathbb{R}^{n_2 \times n_2}, \\ T_M &= \text{diag}(\tau_{M_i}) \in \mathbb{R}^{n_2 \times n_2}, \quad K_M = \text{diag}(k_{M_i}/R_i) \in \mathbb{R}^{n_2 \times n_2}, \end{aligned}$$

the error dynamics of (2.1), (2.8), (2.9) are given in reduced coordinates $x = \text{col}(\theta, \tilde{\omega}, \tilde{\Phi}) \in \mathbb{R}^{(2n-1+n_2)}$ by

$$\begin{aligned} \dot{\theta}(t) &= \mathcal{C}_1 \tilde{\omega}_h + \mathcal{C}_2 \tilde{\omega}, \\ T_P \dot{\tilde{\omega}}(t) &= -\tilde{\omega}(t) - K_P P(\delta(\theta)) + K_P E K_C \tilde{\Phi}_g + c, \\ T_M \dot{\tilde{\Phi}} &= -\tilde{\Phi} - K_M E^\top \tilde{\omega}_h. \end{aligned} \quad (2.11)$$

Here, we have defined, with $P_i(\delta(\theta))$ given in (2.10),

$$\begin{aligned} P(\delta(\theta)) &= \text{col}(P_i(\delta(\theta))) \in \mathbb{R}^n, \\ \tilde{\omega}_h &= \text{col}(\tilde{\omega}_k(t-h_k)) \in \mathbb{R}^n, \quad \tilde{\Phi}_g = \text{col}(\tilde{\Phi}_l(t-g_l)) \in \mathbb{R}^{n_2}, \\ \mathcal{C}_1 &= \mathcal{C} \begin{bmatrix} I_{n_1} & 0_{n_1 \times n_2} \\ 0_{n_2 \times n_1} & 0_{n_2 \times n_2} \end{bmatrix}, \quad \mathcal{C}_2 = \mathcal{C} - \mathcal{C}_1. \end{aligned}$$

Clearly, with Assumption 2.3, the system (2.10), (2.11) possesses an equilibrium point $x^s = \underline{0}_{(2n-1+n_2)}$, the asymptotic stability of which implies asymptotic convergence of all trajectories of the system (2.1), (2.8), (2.9), $i \sim \bar{n}$, to the synchronized motion (up to a uniform shift of all angles).

We are interested in the following problem.

Problem 2.4. *Consider the system (2.1), (2.8), (2.9), $i \sim \bar{n}$, with Assumption 2.3. Given \bar{h}_i , $i \sim \bar{n}$, \bar{g}_i and d_i , $i \sim \bar{n}_2$, derive conditions, such that the corresponding equilibrium point of (2.10), (2.11) is (locally) asymptotically stable.*

3. A class of port-Hamiltonian systems with delays

To address Problem 2.4 and by following [34], we note that with $x = \text{col}(\theta, \tilde{\omega}, \tilde{\Phi}) \in \mathbb{R}^{(2n-1+n_2)}$ the system (2.10), (2.11) can be written as a perturbed pH system with delays

$$\dot{x} = (\mathcal{J} - \mathcal{R})\nabla H + \sum_{i \sim \bar{n}} \mathcal{T}_i (\nabla H_{h_i} - \nabla H) + \sum_{k \sim \bar{n}_2} \mathcal{F}_k (\nabla H_{g_k} - \nabla H), \quad (3.1)$$

with Hamiltonian $H : \mathbb{R}^{(2n-1+n_2)} \rightarrow \mathbb{R}$

$$H = \sum_{i \sim \bar{n}} \frac{\tau_{P_i} \tilde{\omega}_i^2}{2k_{P_i}} - \sum_{i \sim \bar{n} \setminus \{n\}} \frac{c_i \theta_i}{k_{P_i}} + \sum_{i \sim \bar{n}_2} \frac{k_{c_i} \tau_{M_i} R_i \tilde{\Phi}_i^2}{2k_{M_i}} - U(\theta), \quad (3.2)$$

$U(\theta) = \frac{1}{2} \sum_{i \sim \bar{n}} \sum_{k \sim \bar{n}_i} a_{ik} \cos(\theta_{ik} + \delta_{ik}^s)$, interconnection matrix

$$\mathcal{J} = \begin{bmatrix} 0_{(n-1) \times (n-1)} & \mathcal{C} K_P T_P^{-1} & 0_{(n-1) \times n_2} \\ -(\mathcal{C} K_P T_P^{-1})^\top & 0_{n \times n} & \mathcal{J}_1 \\ 0_{n_2 \times (n-1)} & -\mathcal{J}_1^\top & 0_{n_2 \times n_2} \end{bmatrix},$$

with $\mathcal{J}_1 = K_P T_P^{-1} E T_M^{-1} K_M$, damping matrix

$$\mathcal{R} = \text{diag}(\underline{0}_{(n-1)}, K_P (T_P^{-2}) \mathbf{1}_n, (K_M K_C^{-1} T_M^{-2}) \mathbf{1}_{n_2})$$

and $\mathcal{T}_i = \mathcal{J} N_i$, $i \sim \bar{n}_1$, $\mathcal{T}_i = N_i \mathcal{J}$, $i \sim \bar{n}_2$, $\mathcal{F}_k = \mathcal{J} N_k$, $k \sim \bar{n}_2$, with $N_i \in \mathbb{R}^{(2n-1+n_2) \times (2n-1+n_2)}$, the $(n-1+i, n-1+i)$ -th entry of N_i is one and all its other entries are zero, $i \sim \bar{n}_1$, respectively the $(2n-1-n_1+i, 2n-1-n_1+i)$ -th entry of N_i is one and all its other entries are zero, $i \sim \bar{n}_2$.

In light of this fact, it is natural to analyze (2.10), (2.11) by exploiting its pH structure (3.1). Consequently, we consider a generic nonlinear time-delay system in perturbed Hamiltonian form

$$\dot{x} = (\mathcal{J}(x) - \mathcal{R}(x)) \nabla H + \sum_{i=1}^m (\mathcal{T}_i (\nabla H_{h_i} - \nabla H)), \quad (3.3)$$

with state vector $x : \mathbb{R}_{\geq 0} \rightarrow \mathbb{R}^n$, $m > 0$ delays $h_i : \mathbb{R}_{\geq 0} \rightarrow [0, \bar{h}_i]$, $\bar{h}_i \in \mathbb{R}_{>0}$, $\dot{h}_i(t) \leq d_i \leq 1$, Hamiltonian $H : \mathbb{R}^n \rightarrow \mathbb{R}$, matrices $\mathcal{J}(x) = -\mathcal{J}(x)^\top \in \mathbb{R}^{n \times n}$, $\mathcal{R}(x) \geq 0 \in \mathbb{R}^{n \times n}$ and $\mathcal{T}_i \in \mathbb{R}^{n \times n}$, $i = 1, \dots, m$. For the following analysis, we consider initial conditions $x_0 \in W[-h, 0]^n$, where $h = \max_{i \sim \bar{n}} \bar{h}_i$, and make the assumption below.

Assumption 3.1. *The system (3.3) possesses an equilibrium point $x^s = \underline{0}_n \in \mathbb{R}^n$.*

Stability conditions for delayed pH systems of the form

$$\dot{x} = (\mathcal{J}(x) - \mathcal{R}(x)) \nabla H + \sum_{i=1}^m \mathcal{T}_i \nabla H_{h_i}, \quad (3.4)$$

where \mathcal{T}_i are arbitrary interconnection matrices and h_i are time-varying delays have been derived in [27, 38, 15, 2]. It is straight-forward to verify that the system (2.10), (2.11) cannot be written in the form (3.4). In addition, the class of systems (3.4) is a special case of the class (3.3). More precisely, the non-delayed part of (3.4) is restricted to the form $(\mathcal{J}(x) - \mathcal{R}(x))$, while the non-delayed part of (3.3) given by $(\mathcal{J}(x) - \mathcal{R}(x) - \mathcal{T}_i)$ allows to consider more general structures. To illustrate this, consider two pH systems and feedback interconnections

$$\begin{aligned} \dot{x}_1 &= (\mathcal{J}_1(x_1) - \mathcal{R}_1(x_1)) \nabla H_1 + \zeta_1 u_1, \\ \dot{x}_2 &= (\mathcal{J}_2(x_2) - \mathcal{R}_2(x_2)) \nabla H_2 + \zeta_2 u_2, \\ y_1 &= \zeta_1^\top \nabla H_1, \quad u_1 = -y_2(t-h(t)), \\ y_2 &= \zeta_2^\top \nabla H_2, \quad u_2 = y_1(t-h(t)), \end{aligned} \quad (3.5)$$

where $h(t)$ is a transmission delay (uniform, for ease of presentation). Then, the resulting closed-loop system is of the form (3.3) with $H = H_1 + H_2$, $\mathcal{R}(x) = \text{diag}(\mathcal{R}_1(x_1), \mathcal{R}_2(x_2))$,

$$\mathcal{J}(x) = \begin{bmatrix} \mathcal{J}_1(x_1) & -\zeta_1 \zeta_2^\top \\ \zeta_2 \zeta_1^\top & \mathcal{J}_2(x_2) \end{bmatrix}, \quad \mathcal{T}_1 = \begin{bmatrix} \underline{0}_{n \times n} & -\zeta_1 \zeta_2^\top \\ \zeta_2 \zeta_1^\top & \underline{0}_{n \times n} \end{bmatrix}.$$

Now, assume the delay $h(t)$ appears only in one of the feedback interconnections of (3.5). Then the closed-loop system also takes the form (3.3), but not that in (3.4).

4. Delay-dependent stability conditions for time-varying delays

This section is dedicated to the stability analysis of pH systems with bounded time-varying delays represented by (3.3). The approach is based on a strict LKF. To streamline our main result, we note that

$$\nabla \dot{H} = \nabla^2 H ((\mathcal{J} - \mathcal{R} - \sum_{i=1}^m \mathcal{T}_i) \nabla H + \sum_{i=1}^m \mathcal{T}_i \nabla H_{h_i}) \quad (4.1)$$

and make the assumption below.

Assumption 4.1. *Consider the system (3.3) with Assumption 3.1. Set $h_i = 0$, $i = 1, \dots, m$. Then, the equilibrium point $x^s = \underline{0}_n$ of the system (3.3) is (locally) asymptotically stable with Lyapunov function $V_1 = H$.*

Our main result is as follows.

Proposition 4.2. *Consider the system (3.3) with Assumptions 3.1 and 4.1. Given $\bar{h}_i \geq 0$ and $d_i \in [0, 1)$, $i = 1, \dots, m$, assume that there exist $n \times n$ matrices $Y > 0$, $R_i > 0$, $Q_i > 0$, $S_i > 0$ and $S_{12,i}$, $i = 1, \dots, m$, such that*

$$\Psi = \begin{bmatrix} \Psi_{11} & \Psi_{12} & \Psi_{13} \\ * & -S - R & R - S_{12}^\top \\ * & * & \Psi_{33} \end{bmatrix} < 0, \quad (4.2)$$

where

$$R = \text{blkdiag}(R_i), \quad S = \text{blkdiag}(S_i), \quad S_{12} = \text{blkdiag}(S_{12,i}),$$

$$\mathcal{W} = \nabla^2 H(\mathcal{J} - \mathcal{R} - \sum_{i=1}^m \mathcal{T}_i), \quad \mathcal{M} = \nabla^2 H \mathcal{I}_{n \times mn},$$

$$\mathcal{B} = [\mathcal{T}_1^\top (R_1 - S_{12,1}) \quad \dots \quad \mathcal{T}_m^\top (R_m - S_{12,m})], \quad (4.3)$$

$$\begin{aligned} \Psi_{11} = & -\mathcal{R} - 0.5 \left(\sum_{i=1}^m \mathcal{T}_i + \sum_{i=1}^m \mathcal{T}_i^\top \right) + \mathcal{W}^\top Y + Y \mathcal{W} \\ & + \sum_{i=1}^m \left(\bar{h}_i^2 (\mathcal{T}_i \mathcal{W})^\top R_i (\mathcal{T}_i \mathcal{W}) + \mathcal{T}_i^\top (S_i + Q_i - R_i) \mathcal{T}_i \right), \end{aligned}$$

$$\Psi_{12} = [\mathcal{T}_1^\top S_{12,1} \quad \dots \quad \mathcal{T}_m^\top S_{12,m}],$$

$$\Psi_{13} = 0.5 \mathcal{I}_{n \times nm} + \left(Y + \sum_{i=1}^m \bar{h}_i^2 ((\mathcal{T}_i \mathcal{W})^\top R_i \mathcal{T}_i) \right) \mathcal{M} + \mathcal{B},$$

$$\begin{aligned} \Psi_{33} = & \text{blkdiag}(- (1 - d_i) Q_i - 2R_i + S_{12,i} + S_{12,i}^\top) \\ & + \sum_{i=1}^m \bar{h}_i^2 (\mathcal{T}_i \mathcal{M})^\top R_i (\mathcal{T}_i \mathcal{M}), \end{aligned} \quad (4.4)$$

and

$$\begin{bmatrix} R & S_{12} \\ * & R \end{bmatrix} \geq 0 \quad (4.5)$$

are feasible in some neighborhood of x^s . Then the equilibrium $x^s = \underline{0}_n$ is (locally) uniformly asymptotically stable for all delays $h_i(t) \in [0, \bar{h}_i]$, where $h_i(t) \leq d_i$. In addition, assume that (4.2) and (4.5) are feasible for $d_i = 1$, respectively $Q_i = \underline{0}_{n \times n}$, $\forall i = 1, \dots, m$. Then $x^s = \underline{0}_n$ is (locally) uniformly asymptotically stable for all fast-varying delays $h_i(t) \in [0, \bar{h}_i]$.

Proof. Inspired by [8, 7, 15], let $h = \max_{i=1, \dots, m} \bar{h}_i$ and consider the LKF $V : \mathbb{R}_{\geq 0} \times W[-h, 0]^n \times L_2(-h, 0)^n \rightarrow \mathbb{R}$,

$$\begin{aligned} V = & V_1 + V_2 + \sum_{i=1}^m (V_{3_i} + V_{4_i} + V_{5_i}), \quad V_1 = H, \\ V_2 = & \nabla H^\top Y \nabla H, \quad V_{3_i} = \bar{h}_i \int_{t-\bar{h}_i}^t (\bar{h}_i + s - t) \sigma_i(s) ds, \\ V_{4_i} = & \int_{t-\bar{h}_i}^t (\mathcal{T}_i \nabla H(s))^\top S_i (\mathcal{T}_i \nabla H(s)) ds, \\ V_{5_i} = & \int_{t-h_i(t)}^t (\mathcal{T}_i \nabla H(s))^\top Q_i (\mathcal{T}_i \nabla H(s)) ds, \end{aligned} \quad (4.6)$$

where $\sigma_i(\cdot) = (\mathcal{T}_i \nabla \dot{H}(\cdot))^\top R_i (\mathcal{T}_i \nabla \dot{H}(\cdot))$, $i = 1, \dots, m$.

Under the made assumptions H is (locally) positive definite around $x^s = \underline{0}_n$ and $\nabla H|_{x^s} = \underline{0}_n$, which implies that V is an admissible LKF for the system (3.3) with equilibrium $x^s = \underline{0}_n$. Let $\zeta \in \mathbb{R}^{(2m+1)n}$,

$$\zeta = \text{col}(\nabla H, \mathcal{T}_1 \nabla H_{\bar{h}_1}, \dots, \mathcal{T}_m \nabla H_{\bar{h}_m}, \mathcal{T}_1 \nabla H_{h_1}, \dots, \mathcal{T}_m \nabla H_{h_m}).$$

The time-derivative of V_1 is given by

$$\dot{V}_1 = \zeta^\top \begin{bmatrix} -\mathcal{R} - 0.5(\mathcal{T}^\top + \mathcal{T}) & 0_{n \times mn} & 0.5 \mathcal{I}_{n \times mn} \\ * & 0_{mn \times mn} & 0_{mn \times mn} \\ * & * & 0_{mn \times mn} \end{bmatrix} \zeta,$$

where $\mathcal{T} = \sum_{i=1}^m \mathcal{T}_i$. With $\nabla \dot{H}$ given by (4.1), \mathcal{W} given in (4.3) and \mathcal{M} given in (4.3), we have that

$$\dot{V}_2 = \zeta^\top \begin{bmatrix} \mathcal{W}^\top Y + Y \mathcal{W} & 0_{n \times mn} & Y \mathcal{M} \\ * & 0_{mn \times mn} & 0_{mn \times mn} \\ * & * & 0_{mn \times mn} \end{bmatrix} \zeta.$$

Next, $\dot{V}_{3_i} = \bar{h}_i^2 \sigma_i(t) - \bar{h}_i \int_{t-\bar{h}_i}^t \sigma_i(s) ds$, where

$$\sigma_i(t) = \zeta^\top \begin{bmatrix} (\mathcal{T}_i \mathcal{W})^\top R_i (\mathcal{T}_i \mathcal{W}) & 0_{n \times nm} & (\mathcal{T}_i \mathcal{W})^\top R_i \mathcal{T}_i \mathcal{M} \\ * & 0_{nm \times nm} & 0_{nm \times nm} \\ * & * & (\mathcal{T}_i \mathcal{M})^\top R_i \mathcal{T}_i \mathcal{M} \end{bmatrix} \zeta,$$

with \mathcal{M} given in (4.3). By following [7],

$$-\bar{h}_i \int_{t-\bar{h}_i}^t \sigma_i(s) ds = -\bar{h}_i \int_{t-\bar{h}_i}^{t-h_i(t)} \sigma_i(s) ds - \bar{h}_i \int_{t-h_i(t)}^t \sigma_i(s) ds. \quad (4.7)$$

The LMI (4.5) is feasible by assumption. Hence, applying Jensen's inequality together with Lemma 1 in [7], see also [26], to both right-hand side terms in (4.7) yields

$$-\bar{h}_i \int_{t-\bar{h}_i}^t \sigma_i(s) ds \leq - \begin{bmatrix} e_{i1} \\ e_{i2} \end{bmatrix}^\top \begin{bmatrix} R_i & S_{12,i} \\ * & R_i \end{bmatrix} \begin{bmatrix} e_{i1} \\ e_{i2} \end{bmatrix}, \quad i = 1, \dots, m,$$

with $e_{i1} = \mathcal{T}_i (\nabla H - \nabla H_{h_i})$, $e_{i2} = \mathcal{T}_i (\nabla H_{h_i} - \nabla H_{\bar{h}_i})$. Thus,

$$\begin{aligned} & \sum_{i=1}^m \left(-\bar{h}_i \int_{t-\bar{h}_i}^t \sigma_i(s) ds \right) \leq \\ & \zeta^\top \begin{bmatrix} -\sum_{i=1}^m (\mathcal{T}_i^\top R_i \mathcal{T}_i) & \Psi_{12} & \mathcal{B} \\ * & -R & R - S_{12}^\top \\ * & * & -2R + S_{12} + S_{12}^\top \end{bmatrix} \zeta, \end{aligned}$$

with $R, S, S_{12}, \mathcal{B}$ and Ψ_{12} defined in (4.3), (4.4). Also,

$$\begin{aligned} \dot{V}_{4_i} = & (\mathcal{T}_i \nabla H)^\top S_i (\mathcal{T}_i \nabla H) - (\mathcal{T}_i \nabla H_{\bar{h}_i})^\top S_i (\mathcal{T}_i \nabla H_{\bar{h}_i}), \\ \dot{V}_{5_i} = & (\mathcal{T}_i \nabla H)^\top Q_i (\mathcal{T}_i \nabla H) - (1 - \dot{h}_i) (\mathcal{T}_i \nabla H_{h_i})^\top Q_i (\mathcal{T}_i \nabla H_{h_i}) \\ & \leq (\mathcal{T}_i \nabla H)^\top Q_i (\mathcal{T}_i \nabla H) - (1 - d_i) (\mathcal{T}_i \nabla H_{h_i})^\top Q_i (\mathcal{T}_i \nabla H_{h_i}). \end{aligned}$$

Consequently, $\dot{V} \leq \zeta^\top \Psi \zeta$, where Ψ is defined in (4.2). As $\Psi < 0$ by assumption, we have that $\dot{V} \leq -\varepsilon \|x(t)\|^2$

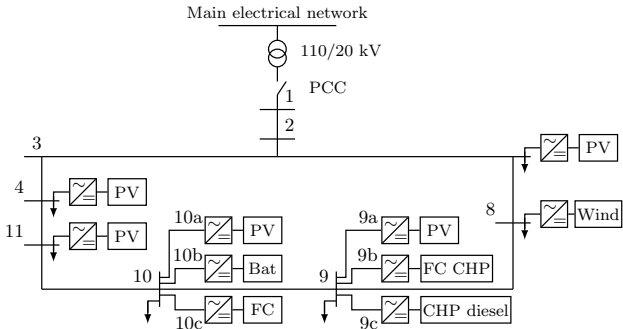


Figure 1: Benchmark model adapted from [29] with 6 main buses, an SG-interfaced combined heat and power (CHP) plant, as well as inverter-interfaced photovoltaic (PV), fuel cell (FC) and battery (Bat) units. PCC denotes the point of common coupling to the main grid. The sign \downarrow denotes loads.

for some $\varepsilon > 0$. Uniform asymptotic stability follows by invoking the LK theorem [7] and arguments from [9] for systems with piecewise-continuous delays.

For the case of purely fast-varying delays, i.e., $d_i = 1$ for all $i = 1, \dots, m$, we see that the negative definite term in \dot{V}_{5_i} vanishes. Hence, by the same arguments as above, if (4.2) is feasible for $d_i = 1$, or equivalently, $Q_i = \underline{0}_{n \times n}$, for all $i = 1, \dots, m$, then $x^s = \underline{0}_n$ is (locally) uniformly asymptotically stable for all fast-varying delays $h_i(t) \in [0, \bar{h}_i]$, completing the proof. $\square\square\square$

Remark 4.3. The conditions given in Proposition 4.2 are, in general, state-dependent. In many cases, the conditions can be conveniently implemented numerically via a polytopic approach [14, 6, 2], see Section 5 of the present paper.

5. Application example: microgrids with distributed rotational and electronic generation

The analysis is illustrated via an example based on the CIGRE benchmark MV distribution network [29]. The network consists of six main buses and is shown in Fig. 1. A combined heat and power (CHP) diesel genset is connected at bus 9c ($i = 4$). The remaining DG units are inverter-interfaced. We assume that the DG units at buses 9b ($i = 1$), 9c, 10b ($i = 2$) and 10c ($i = 3$) are operated with droop control, while all other sources are operated in PQ-mode, i.e., their power injections are regulated to prespecified values [36]. To each droop-controlled unit a power rating is associated, i.e., $S^N = [0.517, 0.333, 0.023, 0.353]$ pu. The parameters for the diesel engine are taken from [28]. We refer the reader to [29] or [34] for a detailed discussion of the employed benchmark model.

5.1. Stability of the non-delayed system

We prove Assumption 4.1 for the system (2.10), (2.11), i.e., that a given equilibrium point of the non-delayed dy-

namics (2.10), (2.11) is locally asymptotically stable with Lyapunov function $V = H$, with H given by (3.2).

Lemma 5.1. Consider the system (2.10), (2.11) with Assumption 2.3. Suppose that $\bar{h}_i = 0$, $i \sim \bar{n}$, $g_k = 0$, $k \sim \bar{n}_2$. The equilibrium point $x^s = \underline{0}_{(2n-1+n_2)}$ of the system (2.10), (2.11) is locally asymptotically stable.

Proof. The stability claim is established via [30, Lemma 3.2.4]. Recall that the system (2.10), (2.11) is equivalent to (3.1). From (3.1) it follows that $\dot{H} = -\nabla H^\top R \nabla H \leq 0$. It is easily verified that $\nabla H|_{x^s} = \underline{0}_{(2n-1+n_2)}$, i.e., x^s is a critical point of H , see also [34, Proposition 5.9]. The Hessian of H is given by

$$\nabla^2 H(x) = \text{blkdiag}\left(\mathcal{L}(\theta), \text{diag}\left(\frac{\tau_{P_i}}{k_{P_i}}\right), \text{diag}\left(\frac{k_{c_i} \tau_{M_i} R_i}{k_{M_i}}\right)\right),$$

where $\mathcal{L} : \mathbb{R}^{(n-1)} \rightarrow \mathbb{R}^{(n-1) \times (n-1)}$, $l_{ii} = \sum_{k \sim \bar{n}} a_{ik} \cos(\theta_{ik} + \delta_{ik}^s)$, $l_{ip} = -a_{ip} \cos(\theta_{ip} + \delta_{ip}^s)$, $i \sim \bar{n} \setminus \{n\}$, $p \sim \bar{n} \setminus \{n\}$. Under the standing assumptions, [34, Lemma 5.8] implies that $\nabla^2 H(x^s) > 0$. Hence, H is locally positive definite and x^s is stable. To prove asymptotic stability, we proceed as in [34] and recall that $\dot{H} \leq 0$, as well as that $R(x) \geq 0$. Hence, x^s is asymptotically stable if—along the trajectories of the system (3.1)—the implication below holds

$$R(x(t)) \nabla H(x(t)) \equiv \underline{0}_{(2n-1+n_2)} \Rightarrow \lim_{t \rightarrow \infty} x(t) = x^s. \quad (5.1)$$

From (5.1) it follows that $\frac{\partial H}{\partial \tilde{\omega}} = \underline{0}_n$, $\frac{\partial H}{\partial \tilde{\Phi}} = \underline{0}_{n_2}$, which implies $\tilde{\omega} = \underline{0}_n$ and $\tilde{\Phi} = \underline{0}_{n_2}$. Hence, θ is constant. Therefore, the invariant set where $\dot{H}(x(t)) \equiv 0$ is an equilibrium. To prove that this is the desired equilibrium $x^s = \underline{0}_{(2n-1+n_2)}$ we recall that x^s is an isolated minimum of $H(x)$, see also Remark 2.2. Thus, there is a neighborhood of x^s where no other equilibrium exists, completing the proof. $\square\square\square$

5.2. Stability of the delayed system

We provide a solution to Problem 2.4 by means of Proposition 4.2. In the present case, the state-dependency of the conditions in Proposition 4.2 is only on the variables θ_i . Note that Ψ defined in (4.2) is continuous in the argument x . Hence, if the stability conditions are verified at an equilibrium x^s , then the local positive definiteness of V given in (4.6) together with the continuity of Ψ in x implies that there exists a small neighborhood $\mathbb{X} \subset W[-h, 0]^{(2n-1+n_2)}$ ($h = \max_{i=1, \dots, m} \bar{h}_i$) of $x_t^s(\sigma) = x^s \in \mathbb{X}$, $\sigma \in [-h, 0]$, such that $V > 0$ and $\dot{V} < 0$, for all $x_t \in \mathbb{X}$, $x_t \neq x^s$. Thus, all trajectories of the system (2.10), (2.11) starting in \mathbb{X} asymptotically converge to x^s .

The Kron-reduced model of the considered μ G possesses 4 nodes. We assume that the fast-varying delays (see Section 2.2) are uniformly upper bounded by $\bar{h}_i = 0.001$ s, $i \sim \bar{n}$. The power-stroke and ignition delay of the diesel engine at node 9c is assumed constant⁵ and initially set

⁵We note that although it is frequently stated in the literature that this delay is time-varying and somewhat dependent on the engine speed, to the best of our knowledge there are no widely-accepted analytic models to represent the time-dependence of this delay.

to $g_4 = 0.125\text{s}$ —the average value in [28], Table 1. The verification of conditions (4.2), (4.5) is done in Yalmip [22].

For this setup, the conditions of Proposition 4.2 are satisfied. Further numerical evaluations show that the equilibrium of the system (2.10), (2.11) is locally asymptotically stable for $g_4 \leq 0.225\text{s}$. Stability for larger values of g_4 can be guaranteed via Proposition 4.2 by reducing the magnitude of the gain $1/R_4$ of the control (2.6) of the SG.

5.3. Region of attraction of the delayed system

It is important to stress that the analysis in Section 5.2 only guarantees stability of an equilibrium for initial conditions within a *small* neighborhood of that equilibrium. Yet in many applications, including μGs , it is often desirable to guarantee stability for a larger set of initial conditions [10]. This can be achieved by providing an estimate of the region of attraction of an equilibrium and, subsequently, verifying conditions (4.2), (4.5) in that whole region rather than just at the equilibrium itself. By following [10], we address this aspect for the MDREG (2.10), (2.11) by exploiting the convexity properties of the Hamiltonian H in (3.2). The lemma below is useful to formulate our result.

Lemma 5.2. *Consider the function $H(x(t))$ in (3.2). Fix a small positive number ϑ , such that $|\theta_{ik} + \delta_{ik}^s| < \frac{\pi}{2} - \vartheta$, $i \sim \bar{n}$, $k \sim \bar{n}_i$ and an arbitrarily large positive number $\beta \gg \vartheta$. The sublevel sets $\Omega_{\mathcal{D}} = \{x \in \mathbb{R}^{(2n-1+n_2)} \mid H(x) \leq c\}$ contained in*

$$\mathcal{D} = \{x \in \mathbb{R}^{(2n-1+n_2)} \mid \|x\| \leq \beta, |\theta_{ik} + \delta_{ik}^s| \leq \frac{\pi}{2} - \vartheta, i \sim \bar{n}, k \sim \bar{n}_i\}. \quad (5.2)$$

are compact.

Proof. The proof follows in an analogous manner to that of [32, Lemma 5.1] and is omitted here for space reasons. $\square\square\square$

Our main result of this section is as follows.

Proposition 5.3. *Consider the system (2.10), (2.11) with Assumption 2.3. Recall the set \mathcal{D} defined in (5.2). Suppose that the equilibrium point $x^s = \underline{0}_{(2n-1+n_2)}$ of the system (2.10), (2.11) is locally asymptotically stable with the LKF $V(x_t, \dot{x}_t)$ defined in (4.6). Let $h = \max_{i=1, \dots, m} \bar{h}_i$ and*

$$\bar{c} = \max_{x \in \mathcal{D}} (H(x)), \quad (5.3)$$

such that the sublevel sets $\Omega_{\mathcal{D}} = \{x \in \mathbb{R}^{(2n-1+n_2)} \mid H(x) \leq \bar{c}\}$ are completely contained in \mathcal{D} . Denote

$$\Omega_c = \{x_h = x(h + \cdot) \in W[-h, 0]^{(2n-1+n_2)} \mid V(x_h, \dot{x}_h) \leq \bar{c}\}.$$

Suppose that $\dot{V} \leq -\epsilon \|x(t)\| \forall x_t \in \Omega_c$ and $t \geq h$. Then, an estimate of the region of attraction of x^s is the set Ω_c .

Proof. To establish the claim, recall that the sublevel sets $\Omega_{\mathcal{D}} = \{x \in \mathbb{R}^{(2n-1+n_2)} \mid H(x) \leq \bar{c}\}$ are completely contained in \mathcal{D} by assumption. Hence, Lemma 5.2 implies

that $\Omega_{\mathcal{D}}$ is a bounded set on which $H(x(t))$ is strongly convex. Furthermore, the strong convexity of H on $\Omega_{\mathcal{D}}$ together with the fact that $\dot{V} \leq 0$ for all $x_t \in \Omega_c$ by assumption implies that $0 \leq V(x_t, \dot{x}_t) \leq V(x_h, \dot{x}_h) \leq \bar{c}$, for all (x_h, \dot{x}_h) such that $V(x_h, \dot{x}_h) \leq \bar{c}$ and \bar{c} given in (5.3). By following [21], we have that $0 \leq H(x(t)) \leq V(x_t, \dot{x}_t) \leq V(x_h, \dot{x}_h) \leq \bar{c}$. Hence, Ω_c is an estimate of the region of attraction of the equilibrium x^s of the system (2.10), (2.11), completing the proof. $\square\square\square$

We provide a solution to Problem 2.4 by means of Propositions 4.2 and 5.3. Recall the Hamiltonian $H(x)$ in (3.2) and that the variables θ_i only appear as arguments of the cosine-function in condition (4.2). Thus, it is straightforward to adopt a polytopic approach, i.e., to represent the set $\{\nabla^2 H(x) \mid x \in \mathcal{D}\}$ as $\nabla H^2 = \sum_{i=1}^q \alpha_i \nabla^2 H^i$, $0 \leq \alpha_i \leq 1$, $\sum_{i=1}^q \alpha_i = 1$, where $\nabla^2 H^i$ denote the vertices of the polytope containing all values that $\nabla^2 H$ can take on the set \mathcal{D} . To ensure asymptotic stability, it then suffices to verify the conditions of Proposition 4.2 for all vertices $\nabla^2 H^i$, see Remark 4.3. The Kron-reduced model of the considered μG possesses 4 nodes. Thus, there are $n(n-1)/2 = 6$ angle differences and the set $\{\nabla^2 H(x) \mid x \in \mathcal{D}\}$ can be fully described with $q = 2^6$ vertices. We set $\vartheta = 10^{-8}$. As before, the implementation of (4.2), (4.5) is carried out with Yalmip [22].

The delays are set to the same values as in Section 5.2. For the nominal configuration with $g_4 = 0.125\text{s}$, the conditions of Proposition 4.2 are satisfied within the whole region \mathcal{D} . Thus, by Proposition 4.2 the considered equilibrium of the system (2.10), (2.11) is locally asymptotically stable and an estimate of its region of attraction is given by Proposition 5.3. Via further numerical evaluations, we verify asymptotic stability of the equilibrium for $g_4 \leq 0.14\text{s}$. As to be expected, this value is considerably lower as that of $g_4 \leq 0.225\text{s}$ obtained in Section 5.2 and illustrates the natural (as in the considered model delays deteriorate the performance) trade-off between the magnitudes of admissible delays and the size of the region of attraction.

5.4. Simulation example

The analysis of Section 5.3 is illustrated via a simulation example. The largest R/X ratio in the Kron-reduced network corresponding to the MDREG in Fig. 1 is 0.30. For high voltage transmission lines it typically is 0.31, see [34]. Hence, the assumption of dominantly inductive admittances is satisfied.

The simulation results in Fig. 2 show that the trajectories of the system (2.10), (2.11) with $\bar{h}_i = 0.001\text{s}$, $i \sim \bar{n}$, and constant $g_4 = 0.14\text{s}$ converge to an equilibrium if conditions (4.2), (4.5) are satisfied. Here, we assumed constant sampling intervals $h_{i,s} = 2 \cdot 10^{-4}\text{s}$, see (2.2). The maximum admissible delay in simulation is $g_4 = 0.155\text{s}$ and, hence, only 1.1 times larger as that of $g_4 = 0.14\text{s}$ derived in Section 5.3. This indicates that our sufficient conditions are very effective for the system under investigation.

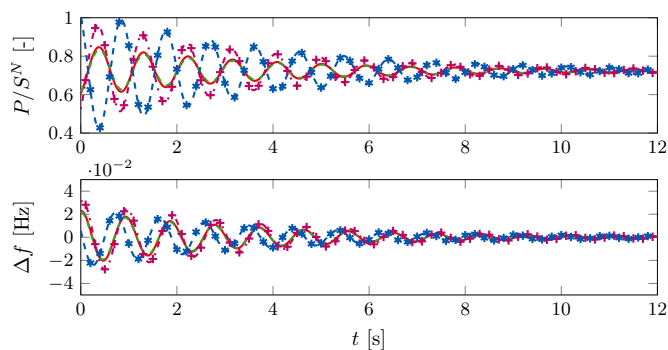


Figure 2: Simulation example of a droop-controlled MDREG with fast-varying delays with $\bar{h}_i = 0.001s$, $i \sim \bar{n}$ and constant power-stroke and ignition delay $g_4 = 0.14s$. Trajectories of the power outputs relative to source rating P_i/S_i^N , and the relative inverter frequencies Δf_i in Hz of the controllable sources. The lines correspond to the following sources: FC CHP 9b, $i = 1$ '—', battery 10b, $i = 2$ '+—' and FC 10c, $i = 3$ '*—', diesel CHP 9c, $i = 4$ '-—'.

6. Conclusions and future work

We have shown that the dynamics of both SG- and inverter-interfaced DG units in μ Gs exhibit time delays. Motivated by this, we have given sufficient delay-dependent conditions for stability of a class of pH systems with delays, which—as a particular case—contains a model of an MDREG. The conditions are derived via a LKF and are valid in the presence of slowly- and fast-varying delays. Furthermore, we have provided an estimate of the region of attraction of an MDREG and the stability conditions have proven to be effective in a practical example. The latter also demonstrates that actuation and power generation delays can, in fact, impair MDREG stability.

In future work, we plan to extend the conducted analysis to further classes of nonlinear systems. With respect to MDREGs, we seek to consider more detailed models of SGs, inverters and network interconnections, e.g., by considering time-varying power lines and variable voltage amplitudes. Furthermore, building upon the presented approaches, we plan to investigate the impact of time delays on communication-based control schemes for μ Gs.

References

- [1] Aoues, S., Lombardi, W., Eberard, D., & Di-Loreto, M. (2015). Stability condition of discrete-time linear Hamiltonian systems with time-varying delay feedback interconnection. *IFAC-PapersOnLine (5th IFAC Workshop on Lagrangian and Hamiltonian Methods for Nonlinear Control)*, *48*, 7–12.
- [2] Aoues, S., Lombardi, W., Eberard, D., & Seuret, A. (2014). Robust stability for delayed port-Hamiltonian systems using improved Wirtinger-based inequality. In *53rd Conference on Decision and Control* (pp. 3119–3124).
- [3] Araposthatis, A., Sastry, S., & Varaiya, P. (1981). Analysis of power-flow equation. *International Journal of Electrical Power and Energy Systems*, *3*, 115–126.
- [4] Efimov, D., Ortega, R., & Schiffer, J. (2015). ISS of multistable systems with delays: application to droop-controlled inverter-based microgrids. In *American Control Conference* (pp. 4664–4669).
- [5] Efimov, D., Schiffer, J., & Ortega, R. (2016). Robustness of delayed multistable systems with application to droop-controlled inverter-based microgrids. *International Journal of Control*, *89*, 909–918.
- [6] Fridman, E. (2014). *Introduction to time-delay systems: analysis and control*. Birkhäuser.
- [7] Fridman, E. (2014). Tutorial on Lyapunov-based methods for time-delay systems. *European Journal of Control*, *20*, 271–283.
- [8] Fridman, E., Dambrine, M., & Yeganehfar, N. (2008). On input-to-state stability of systems with time-delay: A matrix inequalities approach. *Automatica*, *44*, 2364–2369.
- [9] Fridman, E., Seuret, A., & Richard, J.-P. (2004). Robust sampled-data stabilization of linear systems: an input delay approach. *Automatica*, *40*, 1441–1446.
- [10] Galaz, M., Ortega, R., Bazanella, A. S., & Stankovic, A. M. (2003). An energy-shaping approach to the design of excitation control of synchronous generators. *Automatica*, *39*, 111–119.
- [11] Guerrero, J., Loh, P., Chandorkar, M., & Lee, T. (2013). Advanced control architectures for intelligent microgrids – part I: Decentralized and hierarchical control. *IEEE Transactions on Industrial Electronics*, *60*, 1254–1262.
- [12] Guzzella, L., & Amstutz, A. (1998). Control of diesel engines. *IEEE Control Systems*, *18*, 53–71.
- [13] Hatziargyriou, N., Asano, H., Iravani, R., & Marnay, C. (2007). Microgrids. *IEEE Power and Energy Magazine*, *5*, 78–94.
- [14] He, Y., Wu, M., She, J.-H., & Liu, G.-P. (2004). Parameter-dependent Lyapunov functional for stability of time-delay systems with polytopic-type uncertainties. *IEEE Transactions on Automatic Control*, *49*, 828–832.
- [15] Kao, C.-Y., & Pasumarthy, R. (2012). Stability analysis of interconnected Hamiltonian systems under time delays. *IET control theory & applications*, *6*, 570–577.
- [16] Krishnamurthy, S., Jahns, T., & Lasseter, R. (2008). The operation of diesel gensets in a CERTS microgrid. In *PESGM-Conversion and Delivery of Electrical Energy in the 21st Century* (pp. 1–8).
- [17] Kuang, B., Wang, Y., & Tan, Y. L. (2000). An H_∞ controller design for diesel engine systems. In *International Conference on Power System Technology* (pp. 61–66). IEEE volume 1.
- [18] Kukrer, O. (1996). Discrete-time current control of voltage-fed three-phase PWM inverters. *IEEE Transactions on Power Electronics*, *11*, 260–269.
- [19] Kundur, P. (1994). *Power system stability and control*. McGraw-Hill.
- [20] Liu, K., & Fridman, E. (2012). Wirtingers inequality and Lyapunov-based sampled-data stabilization. *Automatica*, *48*, 102–108.
- [21] Liu, K., & Fridman, E. (2014). Delay-dependent methods and the first delay interval. *Systems & Control Letters*, *64*, 57–63.
- [22] Löfberg, J. (2004). YALMIP : a toolbox for modeling and optimization in MATLAB. In *IEEE International Symposium on Computer Aided Control Systems Design* (pp. 284–289).
- [23] Maksimovic, D., & Zane, R. (2007). Small-signal discrete-time modeling of digitally controlled PWM converters. *IEEE Transactions on Power Electronics*, *22*, 2552–2556.
- [24] Münz, U., & Metzger, M. (2014). Voltage and angle stability reserve of power systems with renewable generation. In *19th IFAC World Congress* (pp. 9075–9080).
- [25] Nussbaumer, T., Heldwein, M. L., Gong, G., Round, S. D., & Kolar, J. W. (2008). Comparison of prediction techniques to compensate time delays caused by digital control of a three-phase buck-type PWM rectifier system. *IEEE Transactions on Industrial Electronics*, *55*, 791–799.
- [26] Park, P., Ko, J. W., & Jeong, C. (2011). Reciprocally convex approach to stability of systems with time-varying delays. *Automatica*, *47*, 235–238.
- [27] Pasumarthy, R., & Kao, C.-Y. (2009). On stability of time delay Hamiltonian systems. In *American Control Conference* (pp. 4909–4914).
- [28] Roy, S., Malik, O., & Hope, G. (1991). An adaptive control scheme for speed control of diesel driven power-plants. *IEEE*

- Transactions on Energy Conversion*, 6, 605–611.
- [29] Rudion, K., Orths, A., Styczynski, Z., & Strunz, K. (2006). Design of benchmark of medium voltage distribution network for investigation of DG integration. In *IEEE PESGM*.
 - [30] van der Schaft, A. (2000). *L2-gain and passivity techniques in nonlinear control*. Springer.
 - [31] van der Schaft, A., & Jeltsema, D. (2014). *Port-Hamiltonian systems theory: an introductory overview*. Now Publishers Incorporated.
 - [32] Schiffer, J., Fridman, E., & Ortega, R. (2015). Stability of a class of delayed port-Hamiltonian systems with application to droop-controlled microgrids. In *54th Conference on Decision and Control* (pp. 6391–6396).
 - [33] Schiffer, J., Goldin, D., Raisch, J., & Sezi, T. (2013). Synchronization of droop-controlled microgrids with distributed rotational and electronic generation. In *52nd Conference on Decision and Control* (pp. 2334–2339).
 - [34] Schiffer, J., Ortega, R., Astolfi, A., Raisch, J., & Sezi, T. (2014). Conditions for stability of droop-controlled inverter-based microgrids. *Automatica*, 50, 2457–2469.
 - [35] Schiffer, J., Ortega, R., Hans, C., & Raisch, J. (2015). Droop-controlled inverter-based microgrids are robust to clock drifts. In *American Control Conference* (pp. 2341–2346).
 - [36] Schiffer, J., Zonetti, D., Ortega, R., Stankovic, A., Sezi, T., & Raisch, J. (2016). A survey on modeling of microgrids—from fundamental physics to phasors and voltage sources. *Automatica*, . Accepted, arXiv preprint arXiv:1505.00136.
 - [37] Simpson-Porco, J. W., Dörfler, F., & Bullo, F. (2013). Synchronization and power sharing for droop-controlled inverters in islanded microgrids. *Automatica*, 49, 2603 – 2611.
 - [38] Yang, R., & Wang, Y. (2010). Stability analysis for a class of nonlinear time-delay systems via Hamiltonian functional method. In *8th World Congress on Intelligent Control and Automation (WCICA)* (pp. 2874–2879).